

Observation of Two Ion-Acoustic Waves in a Two-Species Laser-Produced Plasma with Thomson Scattering

S. H. Glenzer, C. A. Back, K. G. Estabrook, R. Wallace, K. Baker, B. J. MacGowan, and B. A. Hammel
L-399, Lawrence Livermore National Laboratory, University of California, P.O. Box 808, Livermore, California 94551

R. E. Cid and J. S. De Groot

Department of Applied Science and Plasma Research Group, University of California, Davis, California 95616
 (Received 30 May 1996)

We report the first observations of two separate ion-acoustic waves in a two-ion-species plasma with Thomson scattering. A flat disk coated with thin multilayers of gold and beryllium was irradiated with one laser beam, and the resulting two-ion-species plasma was probed with a second laser at a distance of $500\ \mu\text{m}$. The phase velocities of the ion-acoustic waves are shown to be a sensitive function of the relative concentrations of the two-ion species. Moreover, an accurate measurement of the ion temperature can be derived from the relative damping of the two-ion-acoustic waves. [S0031-9007(96)00888-5]

PACS numbers: 52.35.Fp, 52.35.Mw, 52.40.Nk, 52.50.Jm

Thomson scattering [1–3] is a powerful plasma diagnostic technique and is widely employed to measure incoherent and collective features of laboratory plasmas [4–6]. Its utility has motivated a large body of theoretical and experimental studies over the last 35 years, principally oriented to single-species plasmas. It is particularly useful for measuring electron plasma and ion-acoustic wave features such as phase velocity and damping which are important for laser-plasma interactions [7,8].

The spectral form factor for Thomson scattering from multispecies plasmas was first derived by Fejer [9], and the influence of impurities on ion-acoustic features in a two-species plasma was specifically calculated by Evans [10]. While the existence of two-ion-acoustic waves in a two-species discharge plasma was demonstrated by measuring two phase velocities with Langmuir probes [11], a successful Thomson scattering experiment testing the predictions of Fejer and Evans has not yet been performed. Besides its importance for plasma diagnostic purposes, a test of the theoretical predictions is of interest for inertial confinement fusion experiments. Many processes affecting the capsule drive in mixed-species fusion plasmas, such as stimulated Raman (SRS) and Brillouin (SBS) scattering, are sensitive to ion wave damping [12,13]. For that reason, it is important that we test our understanding of ion-acoustic waves in such plasmas.

In this Letter, we present Thomson scattering measurements of two-species plasmas consisting of a heavy (Au) and a light (Be) species. For this experiment the solution of the kinetic dispersion relation gives a slow ion-acoustic mode that belongs to the heavy species and a fast ion-acoustic mode belonging to the light species [14]. For small concentrations of heavy species in the plasma, the phase velocity of the slow ion-acoustic mode is a sensitive function of the number fraction and mean charge Z of the heavy species. The phase velocity of the fast mode, on

the other hand, is only slightly affected by the presence of small amounts of heavy ions. We provide a critical experimental test of these predictions by measuring the Thomson scattered spectra for various concentrations of the heavy species and comparing the experimental spectra with theoretical calculations.

The experiments were performed with the Nova laser facility at the Lawrence Livermore National Laboratory. It is a Nd:glass laser operating at $1.055\ \mu\text{m}$ (1ω) which can be frequency converted to 2ω or 3ω . The plasma was produced by illuminating a flat 2 mm diameter disk with a $f/4.3$ laser beam at an angle of 64° to the disk normal. We used a 1 ns square pulse and 2.9 kJ energy at 3ω ($\lambda = 351\ \text{nm}$). A diverging focus resulted in an intensity of $I = 10^{15}\ \text{W cm}^{-2}$ on target. We measured the spot size of $350 \times 800\ \mu\text{m}^2$ by two-dimensional plasma x-ray imaging with a temporal resolution of 80 ps. The disks were coated with Au and Be multilayers of varying thickness. For example, we used 860 layers of 0.5 nm Au and 5.6 nm Be with a total thickness of $2.6\ \mu\text{m}$ on a $51\ \mu\text{m}$ thick Au or $254\ \mu\text{m}$ thick Be substrate to obtain a plasma consisting of 4% Au and 96% Be.

We performed two-dimensional simulations of this experimental configuration with the hydrodynamic code LASNEX [15]. After the beginning of the heating pulse, which is denoted with t_0 , the plasma expands with supersonic speed $v \approx 7 \times 10^7\ \text{cm/s}$. Calculations show that the gold and beryllium ions mix and produce a two-species plasma for distances larger than $z = 30\ \mu\text{m}$ from the target due to ion-ion diffusion. At a distance of $500\ \mu\text{m}$ from the target, the predicted electron temperatures and densities are about 2 keV and $2.5 \times 10^{20}\ \text{cm}^{-3}$ at the end of the heating pulse. When the heater beam turns off at $t = t_0 + 1\ \text{ns}$, the plasma cools rapidly. At $t = t_0 + 1.7\ \text{ns}$, the simulations predict a temperature and density of about 500 eV and $2 \times 10^{20}\ \text{cm}^{-3}$. In addition, recombination

of the plasma reduces the mean charge state Z of the gold ions from about 51 at the end of the heating pulse to about 45 at $t = t_0 + 1.7$ ns. For $t > t_0 + 1$ ns and distances from the target larger than $200 \mu\text{m}$, the temperature and velocity gradients are small. On a spatial scale of $L = 200 \mu\text{m}$ they are calculated to be $(L/T)dT/dz < 10\%$ and $(L/v)dv/dz < 20\%$, respectively.

Thomson scattering was performed at a distance of $z = 500 \mu\text{m}$ from the disk (Fig. 1). The probe laser was parallel to the disk and focused to $200 \mu\text{m}$ diameter. The scattering volume was a cylinder with $150 \mu\text{m}$ length. The probe laser was operating at 2ω ($\lambda = 526.6 \text{ nm}$) with an energy of 100 J in a 4 ns square pulse, resulting in an intensity of $I = 8 \times 10^{13} \text{ W cm}^{-2}$. The experiments showed no effect of the probe laser on the plasma conditions for probe laser intensities up to $I = 3 \times 10^{14} \text{ W cm}^{-2}$. This result agrees with the simulations which show no effect for $t_0 < t < t_0 + 1.7$ ns because the energy delivered by the probe during this time is less than 1% of the heater beam.

The scattered light was imaged at a scattering angle of $\theta = 104^\circ$ with $f/10$ optics and a 1:1.5 magnification onto the entrance slit of a 1 m spectrometer (Spex, model 1704). An optical streak camera (S-20) was used to record spectra with 30 ps temporal resolution. The spectrometer employed a 2400 g/mm grating blazed at 500 nm , resulting in a reciprocal linear dispersion of 0.220 nm/mm (first order). The wavelength resolution of the measurements was 0.1 nm . Wavelength calibration and absolute calibration of the detection system were performed with a Ne spectral lamp and a tungsten lamp.

Collective Thomson scattering is expected for the parameters of the experiment (electron density, temperature, scattering angle, and probe laser wavelength). The scattering parameter $\alpha = 1/k\lambda_D > 3$, and light is predominantly scattered into the narrow ion feature of the

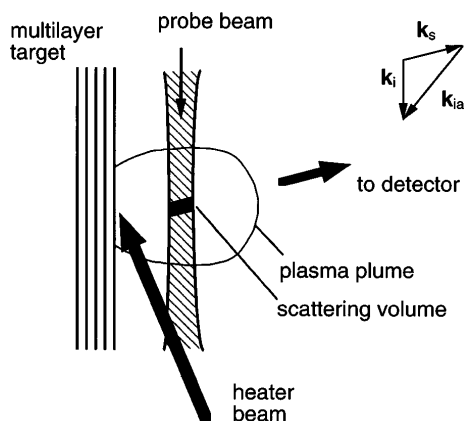


FIG. 1. Scheme of the experimental setup. The angle between the incident heater beam and the disk normal is 64° and the scattering angle between the probe beam and the direction of observation is 104° . The projection of the heater beam on the target plane is 97° to the probe beam.

Thomson scattering spectrum. In this regime, the spectrum of a single species plasma shows two-ion-acoustic features (redshift and blueshift for copropagating and counterpropagating ion-acoustic waves). The frequency separation of the ion-acoustic features is twice the ion-acoustic frequency, and the propagation direction of the corresponding ion-acoustic waves in the plasma is determined by the scattering vector \mathbf{k} , $\mathbf{k} = \mathbf{k}_i - \mathbf{k}_s$. The incident wave vector is defined by $\mathbf{k}_i = (2\pi/\lambda_i)\mathbf{e}_i$, where λ_i is the incident probe laser wavelength and \mathbf{e}_i is the unit vector in direction of the probe laser. Similarly, \mathbf{k}_s points in the direction of the detector (Fig. 1). For a two-species plasma with two ion-acoustic waves (each with redshift and blueshift), the Thomson scattering will show four ion-acoustic features.

Figure 2 shows an example of the recorded Thomson scattered spectrum for a 4% Au, 96% Be target. Four ion-acoustic features, the two outer ones belonging to Be and the two inner ones belonging to Au, can be clearly seen for $t_0 + 0.9 \text{ ns} < t < t_0 + 1.7 \text{ ns}$. The 3ω heater beam lasts from 0 to 1 ns and the 2ω probe beam from 0 to 4 ns . The Thomson scattering signal is fairly symmetric and starts at $t = t_0 + 800 \text{ ps}$. It shows an increasing separation of the ion-acoustic features for about 200 ps , indicating increasing temperatures of the plasma during the heating period. After the end of the heating at $t = t_0 + 1 \text{ ns}$, the separation of the ion-acoustic features decreases rapidly since the plasma cools due to radiative cooling and expansion. For the time interval shown in Fig. 2, Thomson scattering gives temperatures of the plasma of $200 < T_e < 900 \text{ eV}$, ensuring that the Be ions

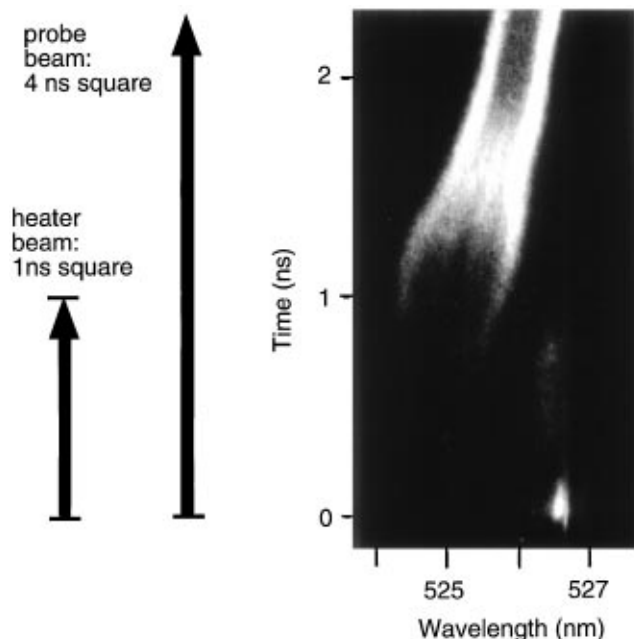


FIG. 2. Time-resolved Thomson scattering spectrum from a 4% Au, 96% Be plasma detected at a distance of $500 \mu\text{m}$ from the target.

are fully ionized. The separation and damping of the ion-acoustic features belonging to the Be ions can be directly used to determine the temperature. In addition, electron densities with an uncertainty of about a factor of 2 are obtained from simulations and the calibration of the detector. This predicts a scattering parameter α well above 3 for our conditions, in which case scattering spectra are not sensitive to the electron density.

The separation of the Au features is indicative of the relative concentration of Au and its charge state. Based on our simulations, we assume that no significant deviations from the 4% Au, 96% Be mixture occur for the first 4 ns of the experiment. Therefore, the temporally resolved scattering allows us to deduce the charge state of the Au ions as a function of time by comparing the separation of the ion-acoustic features of Au and Be. We find a mean Au charge state of 49 at $t = t_0 + 1$ ns decreasing to 40 at $t = t_0 + 1.7$ ns. For later times, $t > t_0 + 1.7$ ns, the charge state of Au further decreases, making it more difficult to identify the ion-acoustic features of Au in Fig. 2.

The early signal detected about 800 ps before the onset of the Thomson scattering signal is due to unconverted 2ω stray light from the heater beam. This feature is not caused by the probe beam and represents a convenient timing and wavelength fiducial. The delay of 800 ps is due to the time needed for ablation and travel of the plasma from the disk surface to the scattering volume. When the plasma reaches the scattering volume, it is moving toward the observer resulting in a blueshift of the Thomson scattering signal. For the present experiment this shift of the scattering signal is very convenient since the scattering signal does not overlap with the unwanted 2ω stray light. The shift yields the instantaneous macroscopic plasma motion along the scattering vector \mathbf{k} . The measured blueshift of 1.7 nm at $t = t_0 + 0.9$ ns corresponds to a velocity of 10^8 cm/s. It is obvious from Fig. 2 that this is well above the sound speed since the shift of the whole Thomson scattering signal is larger than half the wavelength separation of the ion-acoustic features. Although supersonic expansion velocities are in agreement with our simulations, the quantitative comparison shows that the experimental expansion velocity is about 35% larger than calculated.

Figure 3(a) shows a spectrum at $t_0 + 1.5$ ns $< t < t_0 + 1.6$ ns. Four ion-acoustic features due to the slow and fast ion-acoustic waves are clearly identified. The small asymmetry indicates that the ion-acoustic waves on the red wing are more enhanced than those of the blue, which might be caused by stimulated Brillouin side scattering of the probe laser or by the heat flux driven return current [16]. Asymmetries of the plasma plume with respect to the target normal, due to the oblique incidence of the heating laser, are probably not important because the ion-acoustic waves measured in this experiment with Thomson scattering have small components in the direction of the heating laser. The experimental data are fit-

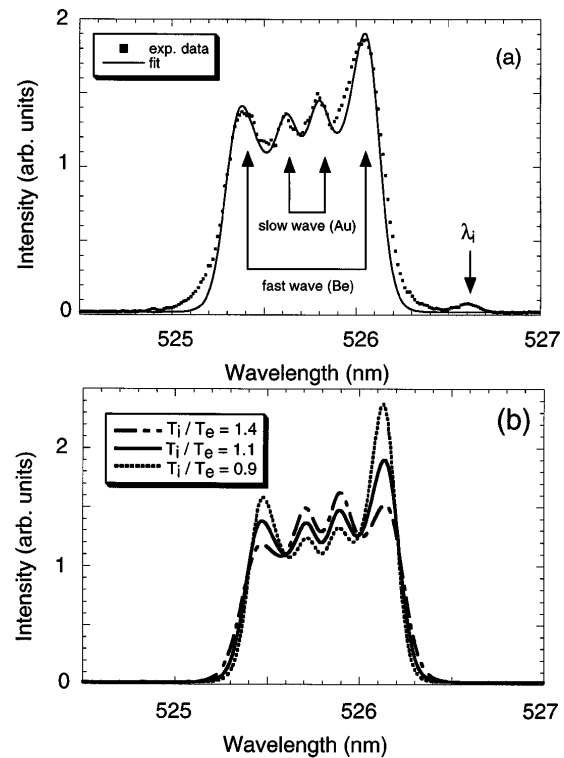


FIG. 3. Thomson scattering spectrum from a 4% Au, 96% Be plasma at $t = t_0 + 1.55$ ns together with a theoretical spectrum for $T_e = 230$ eV, $T_i = 260$ eV, $\alpha = 7$, and $Z_{Au} = 40$ (a). λ_i denotes the incident probe wavelength. Also shown is the variation of the scattering spectrum for various ratios of T_i/T_e (b).

ted with a theoretical spectrum which compensates for the asymmetry by slightly decreasing the damping of the waves on the red wing [5,17]. Apart from the slight asymmetry, analysis of the spectrum yields considerable information. Since the relative intensities of the ion-acoustic features are determined by damping of the Au and Be ion-acoustic waves, the theoretical fit to the spectrum gives $T_i/T_e = 1.1$ [Fig. 3(b)]. From the wavelength separation of the Be ion-acoustic features, we find $T_e = 230$ eV. We can then infer $\alpha = 7$ for the electron densities calculated in the simulations. Finally, the wavelength separation of the Au features gives $Z = 40$. As can be seen, the theoretical spectrum fits the experimental data quite well. Small deviations are probably due to small plasma parameter gradients within the scattering volume.

For the whole duration of the experiment, we find the measured electron temperature and ion-to-electron temperature ratio a factor of about 2 larger than calculated. This is consistent with the measured slightly lower charge state of the Au ions. These results are further consistent with the experimental expansion energy being twice as large as calculated. Further experiments and simulations will be required to resolve these discrepancies.

Figure 4 shows the compilation of our experiments with relative Au concentrations of 1%, 2%, 4%, and 9%. For very small Au concentrations of 1%, the Thomson scattering signal shows a central peak belonging to the heavy Au ions in addition to the ion-acoustic waves belonging to the Be ions. The existence of a central peak was also observed in a two-species discharge plasma consisting of hydrogen and small amounts of heavy gases [17,18]. Increasing the amount of the Au species of the two-species plasma results in a larger separation of the ion-acoustic features of Au. For the 2% case the ion-acoustic waves of Au become discernible as two individual peaks on the spectrum. For a mixture of 4% Au, 96% Be two separate ion-acoustic waves were clearly observed (Fig. 2). By further increasing the amount of Au to 9%, the ion-acoustic waves of Au and Be almost merge together. The plot in Fig. 4 shows the ratio of the wavelength separation of the Au ion-acoustic features to the Be ion-acoustic features as a function of the Au concentration. These data are taken at $t = t_0 + 1.55$ ns when the intensity of the Au features is at its maximum. From the theoretical fit of the spectra we find that T_i/T_e , the scattering parameter α , and charge state Z of the Au ions are the same for all experiments to within 15%. The experimental data clearly show the increase of the wavelength separation of the Au ion-acoustic feature with increasing concentration. The theoretically calculated results [10] are also plotted for various Z of the Au ions. The experimental data are in excellent agreement with the theory for $Z = 40$, which also compares quite well with the calculated value of $Z = 45$.

In contrast to the results shown in Ref. [11] where the phase velocity of the ion-acoustic wave of the heavy species approaches a constant value for small concentrations, the ratio of the present study decreases to zero for small concentrations of the heavy species

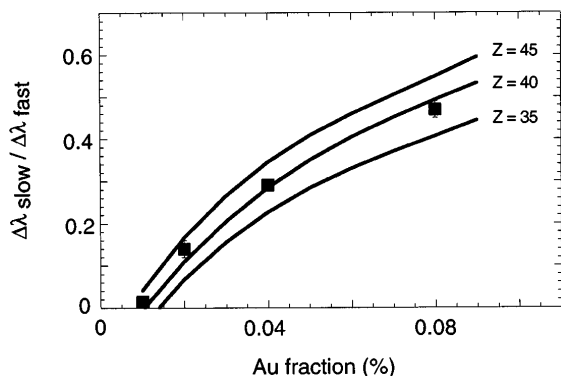


FIG. 4. Ratio of the wavelength separations of the ion-acoustic features belonging to Au to those belonging to Be on the Thomson scattering signal for different Au concentrations. The ratios were taken at $t = t_0 + 1.55$ ns when $T_i/T_e \approx 1.1$ and $\alpha \approx 7$. The error bars are estimated from the noise of the data. Theoretical data after Evans [10] are shown for $Z_{\text{Au}} = 35, 40, 45$.

in the two-species mixture. This result shows that the consideration of the phase velocities of the ion-acoustic waves alone is not sufficient to describe the Thomson scattering spectrum; the complete form factor as given by Evans [10] must be applied. In particular, the observation of both the fast and the slow wave on the Thomson scattering spectra shows that they are moderately to strongly damped. In this regime, Landau damping is a strong function of the ion temperature, resulting in a highly accurate ion temperature measurement.

In summary, we have presented the first measurements of two-ion-acoustic waves in a two-ion-species plasma with Thomson scattering. Our results are in excellent agreement with the theory of Fejer [9] and Evans [10]. We have shown that Thomson scattering from a two-ion-species plasma is an accurate diagnostic of electron temperature and ion temperature. In addition, the relative ion densities can be measured with high accuracy if the ion charge state is known independently or vice versa. Thomson scattering will be a powerful diagnostic to understand SBS and SRS spectra of multispecies plasmas.

We would like to thank the Nova crew for their efforts and E. A. Williams and A. Offenberger for discussions. This work was performed under the auspices of the U.S. Department of Energy by the Lawrence Livermore National Laboratory under Contract No. W-7405-ENG-48.

- [1] E. E. Salpeter, *Phys. Rev.* **120**, 1528 (1960).
- [2] J. A. Fejer, *Can. J. Phys.* **38**, 1114 (1960).
- [3] J. P. Dougherty and D. T. Farley, *Proc. R. Soc. Ser. A* **259**, 79 (1960).
- [4] H.-J. Kunze, in *Plasma Diagnostics*, edited by W. Lochte-Holtgreven (North-Holland, Amsterdam, 1968), p. 550.
- [5] D. E. Evans and I. Katzenstein, *Rep. Prog. Phys.* **32**, 207 (1969).
- [6] J. Sheffield, *Plasma Scattering of Electromagnetic Radiation* (Academic, New York, 1975).
- [7] W. L. Kruer, *The Physics of Laser Plasma Interactions* (Addison-Wesley, New York, 1988).
- [8] T. P. Hughes, *Plasmas and Laser Light* (John Wiley and Sons, New York, 1975).
- [9] J. A. Fejer, *Can. J. Phys.* **39**, 716 (1961).
- [10] D. E. Evans, *Plasma Phys.* **12**, 573 (1970).
- [11] Y. Nakamura *et al.*, *Phys. Rev. Lett.* **37**, 209 (1976).
- [12] B. J. MacGowan *et al.*, *Phys. Plasmas* **3**, 2029 (1996).
- [13] R. K. Kirkwood *et al.*, *Phys. Rev. Lett.* **76**, 2065 (1996).
- [14] B. D. Fried *et al.*, *Phys. Fluids* **14**, 2388 (1971); R. J. Huck and E. A. Johnson, *Phys. Rev. Lett.* **44**, 142 (1980); E. A. Williams *et al.*, *Phys. Plasmas* **2**, 129 (1995).
- [15] G. Zimmerman and W. Kruer, *Comments Plasma Phys. Controlled Fusion* **2**, 85 (1975).
- [16] J. S. De Groot *et al.*, *AIP Conference Proceedings No. 318* (Plenum Press, New York, 1994), p. 135.
- [17] Th. Wrubel *et al.*, *J. Atmos. Terr. Phys.* **58**, 1077 (1996).
- [18] A. W. DeSilva *et al.*, *Phys. Fluids B* **4**, 458 (1992).